Adv. Radio Sci., 9, 383–389, 2011
www.adv-radio-sci.net/9/383/2011/
doi:10.5194/ars-9-383-2011

Advances in Radio Science

Advanced parametrical modelling of 24 GHz radar sensor IC packaging components

R. Kazemzadeh[1], W. John[2], J. Wellmann[1], U. B. Bala[1], and A. Thiede[1]

[1]University of Paderborn (HFE), Paderborn, Germany
[2]Leibniz University Hannover (TET), Hannover/SIL R+D, Paderborn, Germany

Abstract. This paper deals with the development of an advanced parametrical modelling concept for packaging components of a 24 GHz radar sensor IC used in automotive driver assistance systems. For fast and efficient design of packages for system-in-package modules (SiP), a simplified model for the description of parasitic electromagnetic effects within the package is desirable, as 3-D field computation becomes inefficient due to the high density of conductive elements of the various signal paths in the package. By using lumped element models for the characterization of the conductive components, a fast indication of the design's signal-quality can be gained, but so far does not offer enough flexibility to cover the whole range of geometric arrangements of signal paths in a contemporary package. This work pursues to meet the challenge of developing a flexible and fast package modelling concept by defining *parametric* lumped-element models for all basic signal path components, e.g. bond wires, vias, strip lines, bumps and balls.

1 Introduction

To obtain the lumped element models for the parametric modelling concept, the parametric simulations of the considered structures are first carried out with 3-D field solvers (like EMPIRE, 2009), where the parameter typically is a geometric quantity, like length, height, diameter, thickness or distance of the structures. Then, the simulation results are used to obtain the lumped-element description of the conductive structure. Section 2 examines the feasibility of the pursued parametric modelling concept by reassembling signal path structures from the parametric lumped element characterizations of the basic conductive components and comparing the results of the lumped element signal path models to those of the 3-D field calculations. Section 3 deals with the modelling of parametric ball structures. Section 4 addresses the parametric modelling of bond wire structures with focus on different numerical tools to minimize the effect of their specific behaviour.

Correspondence to: W. John
(john@tet.uni-hannover.de)

2 Parametric modelling of vertical interconnect structures

This section addresses the issue whether it is possible to characterize the electromagnetic behaviour of a package signal path by interconnection of RLC models of the basic signal path elements, like vias, bond wires, balls, strip lines or combinations of these. To verify the feasibility of the pursued parametrical modelling concept, as a first step only the via inductance is being focused on, neglecting the coupling capacitance between the via-body and the P/G-planes according to the equivalent circuit model of a via in Fig. 1.

The examination of via-configurations in conjunction with signal lines shows that the characteristic behaviour of such a configuration, e.g. the impedance characteristic, cannot be approximated by simple interconnection of the RLC models.

For instance, the characteristic of a via with a via length of $l_{\mathrm{ViaBody}} = 100\,\mu\mathrm{m}$ and micro strip length of $l_{\mathrm{Microstrip}} = 50\,\mu\mathrm{m}$, secluding at the upper and lower via pad, cannot simply be characterized by an interconnection of the RLC models of e.g. a via with $l_{\mathrm{ViaBody}} = 50\,\mu\mathrm{m}$ in conjunction with a micro strip of $l_{\mathrm{Microstrip}} = 50\,\mu\mathrm{m}$ and another via with $l_{\mathrm{ViaVody}} = 50\,\mu\mathrm{m}$. Hence, the RLC models of the individual elements (via, ball, bond wire etc.) are not suitable as basic models for the pursued modelling concept, since the occurring effects at the interfaces of the interconnected elements are not being regarded. The consideration of these effects would require modelling them individually. Here, a different approach is followed by using combinations of the individual

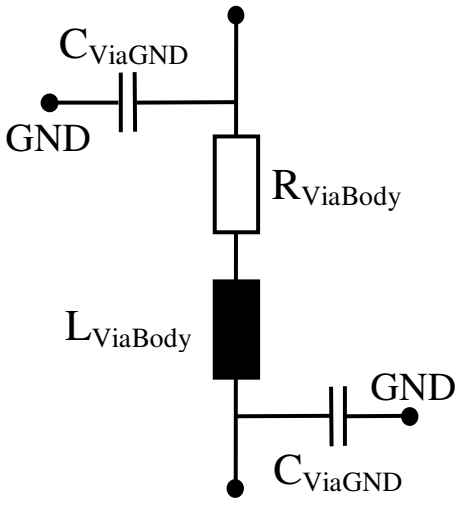

Fig. 1. Equivalent circuit model of a via.

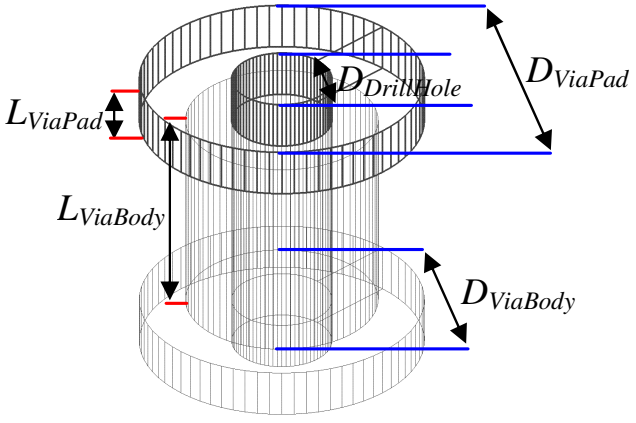

Fig. 2. Graphical representation of a via.

signal path elements as basic RLC models. More precisely, a via in conjunction with micro strip lines at its upper and lower pad serves as a basic model, allowing the consideration of transition effects at the micro strip/via-pad junction. Using a 3-D FDTD solver for all electromagnetic field simulations, a simple signal path arrangement consisting of three vertically interconnected vias with micro strip lines at the very upper and very lower via-pad is being examined. As can be expected, this signal path arrangement shows nearly the same impedance characteristic as a single via of the same overall via length and micro strip length. Fig. 3 shows the inductance L_{SP} of the considered signal path arrangement as a function of its overall vertical length l_{Vertical}.

Here, the inductance of the single vias in conjunction with signal lines is represented by continuous lines, whereas the inductance of the simple signal path arrangement of three vertically connected vias in conjunction with signal lines is shown by the dashed lines. As the capacitive via-GND cou-

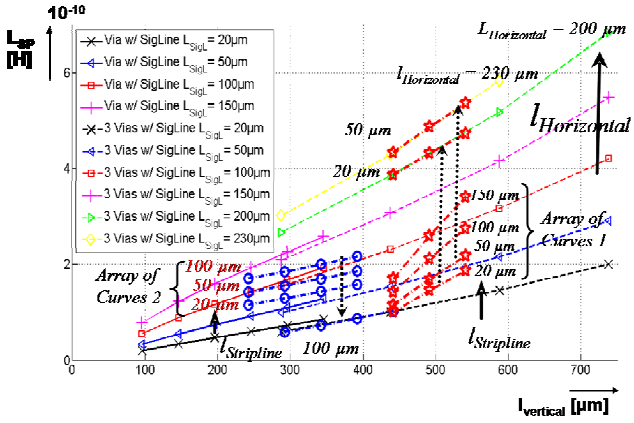

Fig. 3. Signal path inductance L_{SP} (vertical and horizontal signal path length for basis model (continuous curves)) – three vertically interconnected vias (dashed) – signal path arrangement (array of curves).

pling is not regarded at this stage, the impedance characteristic can be approximated from the inductance values displayed in Fig. 3, since the loss resistance of the considered arrangements is negligible. The second parameter, besides the vertical overall length l_{Vertical} of the signal path arrangements, is the horizontal signal line length $l_{\mathrm{Horizontal}}$. Ascending in the direction of the ordinate, each curve represents an arrangement with a constant signal line length, as indicated in the legend of Fig. 3 and as assigned at the array of curves in the same figure. The inductance of the arrangements of vias grows nearly linearly with increasing via length. Furthermore, the inductance increases with the signal line length. Comparing the dashed curves for the three via arrangement, an increase in signal line length involves an increase of the gradient for the respective curve. Since the inductance increases nearly linearly with the via length and the gradient of the curves rises nearly linearly with the signal line length, every point in the considered space or, respectively, within the considered geometric domain for the signal path arrangements can be approximated by means of simple algorithms.

To further verify the parametric modelling concept, in a next step a benchmark signal path example is established to see if it is possible to approximate its impedance characteristic by interconnection of variations of the basic via/signal line model.

Figure 4a–d shows the signal path example consisting of three vias, two of which are positioned above each other, with the third via positioned on the level of the gap between the two vias, but laterally displaced. The three vias are interconnected with strip lines according to Fig. 4. Four geometric parameters are analyzed: The length of the strip lines $l_{\mathrm{Stripline}}$ between the middle via and the upper/lower via (Fig. 4a), the length of the micro strip $l_{\mathrm{Microstrip}}$ at the upper/lower via (Fig. 4b), the length of the middle via-body l_{MidVia} (Fig. 4c) and the length of the lower via-body

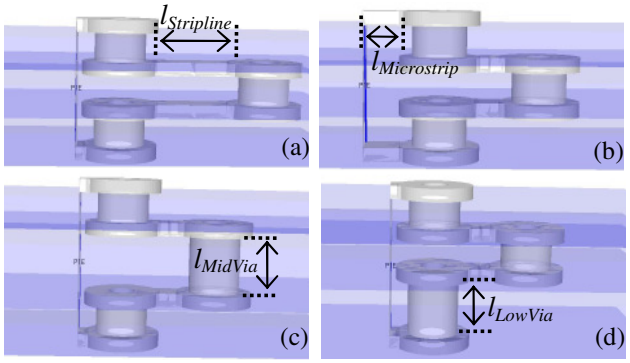

Fig. 4. Investigated signal path arrangement with examined parameters: **(a)** strip line length $l_{\text{Stripline}}$ – **(b)** micro strip length $l_{\text{Microstrip}}$ – **(c)** middle via-body length l_{MidVia} – **(d)** lower via body length l_{LowVia}.

l_{LowVia} (Fig. 4d). The range of variation of the geometric parameters for the signal path arrangement is listed in Table 1, in addition to the other via and signal line parameters. An illustration of the via parameters is given in Fig. 2. First, the variation of the middle via-body length $l_{\text{Microstrip}}$ in conjunction with the strip line length $l_{\text{Stripline}}$ was analyzed (Fig. 4a/c), where the length of the upper and lower via-body is $l_{\text{UpVia}}, l_{\text{LowVia}} = \text{const.} = 50\,\mu\text{m}$ and the length of the micro strip is $l_{\text{Microstrip}} = \text{const.} = 20\,\mu\text{m}$.

The results, displayed by the array of curves 1, were displaced 200 units in the direction of the abscissa to not overlay with the array of curves 2 in Fig. 3. It is apparent that the curves of array 1 have a higher gradient compared to the rest of the curves. As mentioned earlier, the gradient of a curve at a certain via length is determined by the length of the signal lines connected to the via. Although the length of the micro strip and the strip line is $l_{\text{Stripline}} - l_{\text{Microstrip}} = 20\,\mu\text{m}$ for the under most curve of the array 1, the gradient is evidently higher than the gradients of the curves for the basic models with the same or even higher signal line lengths. Moving the two under most curves of array 1 onto the curves for the three vertically interconnected vias in conjunction with signal line lengths $l_{\text{Horizontal}} = 200\,\mu\text{m}$ and $l_{\text{Horizontal}} = 230\,\mu\text{m}$ shows the same gradients for each pair of curves, as delineated in Fig. 3. Thus, the considered signal path arrangement behaves like a basic model with considerably longer signal lines. Comparing the signal path arrangement to the basic model of the same length, the former possesses additional horizontal conductors, which are the lower via pad of the upper via and the upper via pad of the displaced via (or, the lower via pad of the displaced via and the upper via pad of the lower via, respectively) (Fig. 4).

Adding the length of these additional horizontal conductors to the overall signal line length of the signal path arrangement, we approximately obtain the signal line length of the basis model with the same gradient as the signal path

Table 1. Parameters of calculated structures.

Characteristic (all Models)	Value	Unit
Height of signal lines/via pads	23	µm
Width of signal lines	65	µm
Diameter of via-pads d_{ViaPad}	142	µm
Diameter of via-body d_{ViaBody}	96	µm
Diameter of drill hole $d_{\text{DrillHole}}$	50	µm
Dielectric constant of substrate material ε_r	3.5	–
Basic Model and Three Vertical Vias Model		
Vertical length l_{Vertical}	96–738	µm
Horizontal length $l_{\text{Horizontal}}$	20–230	µm
Signal Path Arrangement		
Middle via-body length l_{MidVia}	50–150	µm
Up/low via-body length $l_{\text{UpVia}} - l_{\text{LowVia}}$	50–150	µm
Overall vertical length l_{Vertical}	242–392	µm
Micro strip length $l_{\text{Microstrip}}$	20–150	µm
Strip line length $l_{\text{Stripline}}$	20–150	µm

arrangement, which explains the agreement of the gradients of the curves. Thus, it is possible to approximate the characteristic of the signal path arrangement for the parameters $l_{\text{Stripline}}$ and l_{MidVia} by means of the basic model. Next, the variation of the lower via-body length l_{LowVia} in conjunction with the strip line length $l_{\text{Stripline}}$ was analyzed (Fig. 4 a/d), where the length of the upper and middle via-body is l_{UpVia} and $l_{\text{MidVia}} = \text{const.} = 50\,\mu\text{m}$ and the length of the micro strip is $l_{\text{Microstrip}} = \text{const.} = 20\,\mu\text{m}$. The results are displayed by the array of curves 2 in Fig. 3. Here, it stand out that the gradients of the curves of array 2 all have the same gradient and that the variation of the strip line length $l_{\text{Stripline}}$ has no effect on the gradient, in contrast to the preceding examination of the strip line length $l_{\text{Stripline}}$ in conjunction with the middle via-body length l_{MidVia}. The gradient of the curves is determined by the length of the micro strip $l_{\text{Microstrip}} = \text{const.} = 20\,\mu\text{m}$, independent of the strip line length $l_{\text{Stripline}}$, which becomes obvious when one of the curves of the curve array 2 is shifted onto the basic model curve for $l_{\text{Microstrip}} = 20\,\mu\text{m}$ (see Fig. 3). The same behaviour is observed for the signal path arrangement with longer micro strip lengths in comparison with the basic model with according horizontal lengths. This leads to the conclusion that the variation of signal line length only effects the gradient, if the signal lines are being varied at both ends of the varied via. Again, it is possible to approximate the behaviour of the signal path arrangement for the parameters $l_{\text{Stripline}} - l_{\text{LowVia}}$ and $l_{\text{Microstrip}}$ by means of the basic model. As an example, based on the former findings, the inductance of a signal path arrangement with an overall vertical length of $l_{\text{Vertical}} = 242\,\mu\text{m}$ according to Fig. 4, a micro strip and strip line length of $l_{\text{Microstrip}} = l_{\text{Stripline}} = 20\,\mu\text{m}$ and a via-body length of $l_{\text{UpVia}} = l_{\text{LowVia}} = l_{\text{MidVia}} = 50\,\mu\text{m}$

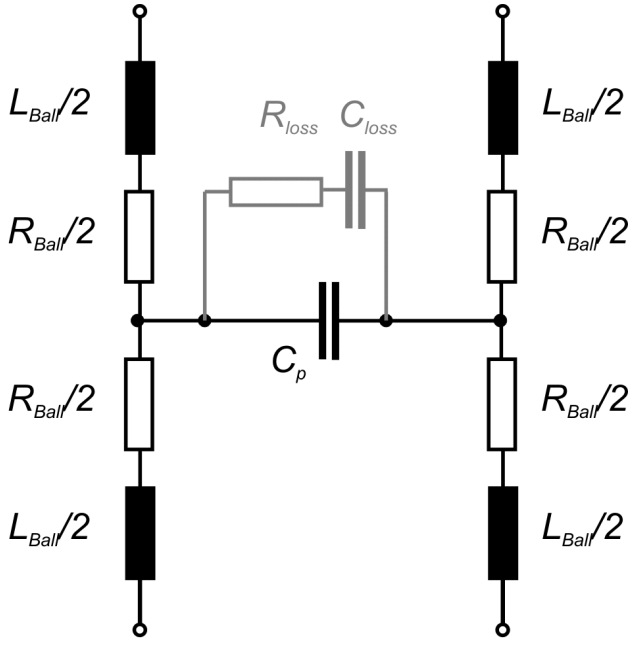

Fig. 5. Equivalent circuit model of two balls and capacitive coupling.

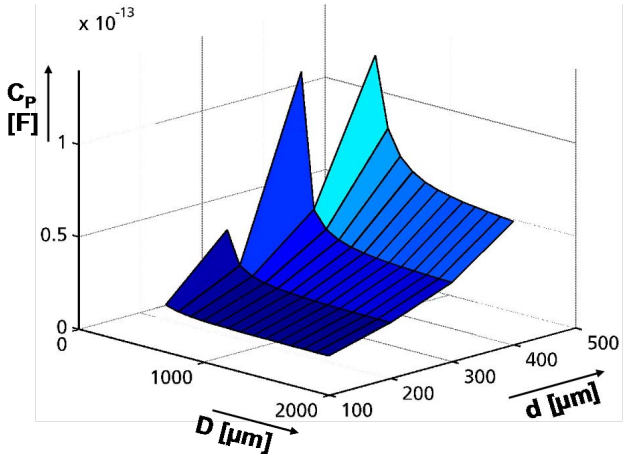

Fig. 6. Ball to ball coupling capacity C_P; $\varepsilon_r = 1$.

can be approximated by a basis model of l_{Vertical}= 242 µm and $l_{\text{Horizontal}} = 20$ µm in conjunction with a basis model of $l_{\text{Vertical}} = 50$ µm and $l_{\text{Horizontal}} = 200$ µm.

3 Parametric modelling of ball-structures

The use of spherical ball- or bump-structures for interconnections between die and interposer (FlipChip/SIP) or BGA packages requires an appropriate way of modelling.

Regarding the ball geometry, tinned bumps of pure solder/tin compounds will form a spherical body after soldering, depending on the amount of material and the height of the connection (Hussein, 1996).

In this work, a simplified geometry was inspected to reduce the number of parameters for the parametrical lumped element model to the overall diameter of the ball. The angles of the cutting-planes are kept constant, giving a diameter of the upper and lower pads relative to the balls diameter.

Different parameters will be used for modelling: The diameter d of the ball, the distance D between two balls, ε_r of the surrounding material and the conductivity σ_r of the ball's material. The dominant non-resistive elements are the inductance of the single ball and the coupling-capacitance between two balls (Fig. 5). For better symmetry, the ball-inductance is splitted in half, so the coupling-network between several bumps can be connected without any vertical mismatch giving a symmetrical model. The inter-bump coupling-network includes, apart from the coupling-capacitance C_p, additional elements to model resistive and dielectric losses.

As shown in Table 3, the parameterization of the inductance between ball and diameter is linear (Ndip, 2003).

The coupling capacitance C_p between two balls (see Fig. 6) dominates the magnetic coupling factor (Ahn, 2000). It should be noted that the distance between two balls is measured between the ball's central points, so $D = d$ would mean a direct contact between the two balls, and an infinity capacitance for $D/d \gg 0$. As shown in Fig. 7, the capacitance converges to a 1/D-behaviour. For getting an approximation for close ball distances it is necessary to use the relative ball distance between central points). The size of the coupling capacity C_p can be approximated as

$$C_p(D,d,\varepsilon_r) \approx \varepsilon_r \varepsilon_o d_2 \frac{k_1 D + k_2}{D - d} \tag{1}$$

where D is the distance between two balls, ε_r the dielectric constant of the underfill, and $k_1 \approx 2.29 \times 10^8$, $k_2 \approx -2.32 \times 10^6$ are fitting parameters.

The dielectric losses of the underfill-material are not part of this parametric model, as no major influence was observed for the inspected materials (Polyimide/Epoxy/Polyclad) in the targeted frequency range up to 30 GHz.

For precise modelling of the dielectric losses for higher frequencies or different materials, additional R and RC-Networks can be connected in parallel to the coupling capacitance C_p.

4 Parametric modelling of bond wire

This section deals with the parametrical modelling of bond wires. The bond wires will be parameterized by varying their length and the distance between two bond wires. In the present model, JEDEC4 bond wires are being considered (Fig. 8), where the height of each bond wire is 200 µm and consists of PEC (Perfectly Electrically Conducting) material. The bond wire radius is 12.5 µm. The substrate is

Table 2. Parameters of calculated structures.

Characteristic	(all Models)	Value	Unit
Diameter d (Ball)		30–480	µm
Diameter (Pad)		$0.8 \times d$	µm
Height (Pad)		24	µm
Distance D (between Balls)		200–1600	µm
Relative permittivity of substrate/underfill material ε_r		2.0/3.5/11.9	–
Conductivity of ball material s_r Tin Gold Copper		$8.67 \times 10^6 4.1 \times 10^7 5.8 \times 10^7$	1/(Ohm×m)

Table 3. Inductance of a single ball.

BallDiameter d	FieldComputation	Parameterization
30 µm	59.5 pH	60 pH
60 µm	65.9 pH	66 pH
90 µm	71.9 pH	72.4 pH
120 µm	77.9 pH	78.3 pH

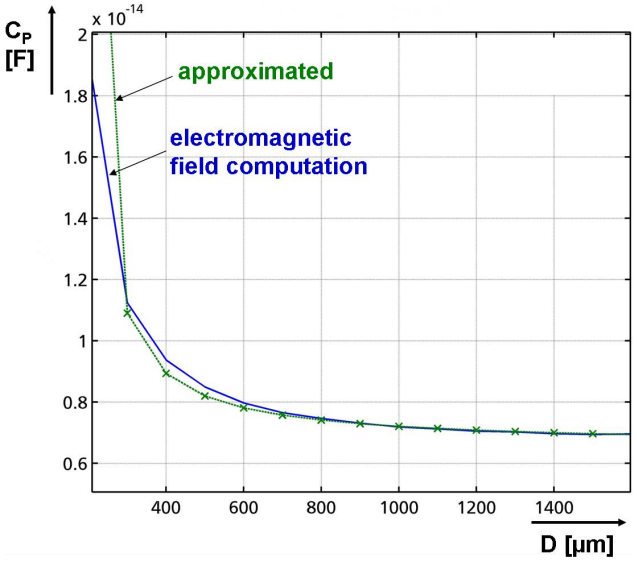

Fig. 7. Coupling capacity C_p (ball distance D; $\varepsilon_r = 1$; $d = 180$ µm.

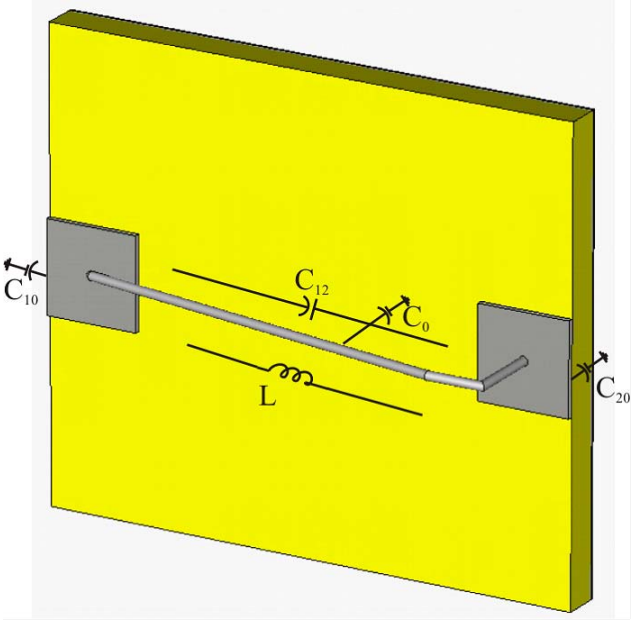

Fig. 8. 3-D model of single bond wire.

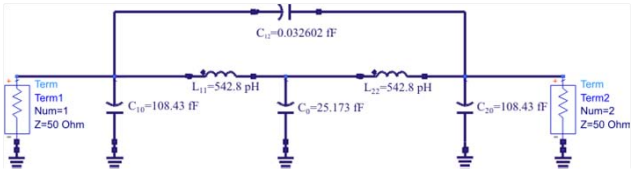

Fig. 9. Equivalent circuit model of a single bond wire.

considered as Silicon (loss free) and the size of each pad is 250 µm × 250 µm × 15 µm.

First of all, a parameterization of the bond wire will be carried out by variation of its length. In order to achieve this, S-parameters are being computed using the 3-D field calculator CST Microwave Studio. The equivalent circuit model of a single bond wire is shown in Fig. 9. Since PEC material is considered, there will be no resistance. The pad to GND capacitances are labelled C_{10} and C_{20} and the capacitance between the pads is labelled C_{12}. The bond wire will be represented as an inductance which is divided into two parts L_{11} and L_{22}, and C_0 represents the capacitance between the bond wire and the GND. Since the result is renormalized with 50 Ohm resistance, two ports with the same resistance are added at the two ends. The values of these parameters are being obtained using Ansoft Q3-D for the length variation of 400 µm to 2000 µm with a step size of 400 µm. The pad to GND capacitance remains constant, $C_{10} = C_{20} = 108.4$ fF. The results of the other parameters are shown in Table 4.

Using these results, the S parameters of this equivalent circuit are calculated with the help of ADS (Advanced Design

Table 4. Different parameters of single bond wire.

Bond Wire Length [µm]	Pad Capacitance C_{12} [fF]	Bond Wire Inductance [pH]	Bond Wire Capacitance C_0 [fF]
400	2.22	0.3297	12.89
800	0.0862	0.6539	20.21
1200	0.0326	1.086	25.17
1600	0.0178	1.39	35.44
2000	0.0112	1.79	43.41

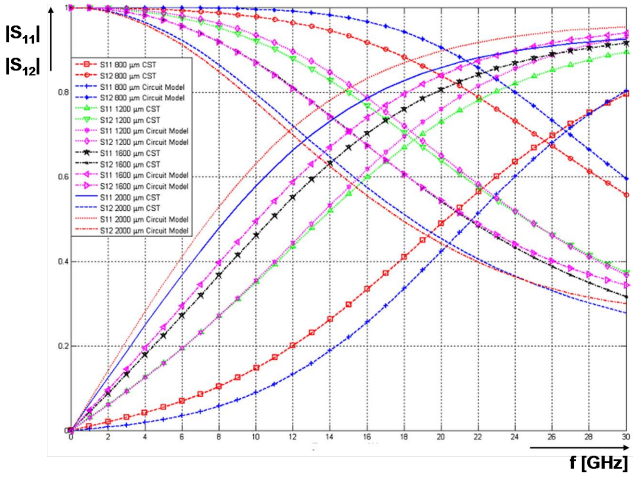

Fig. 10. Comparison of S parameters of a single bond wire with varying length.

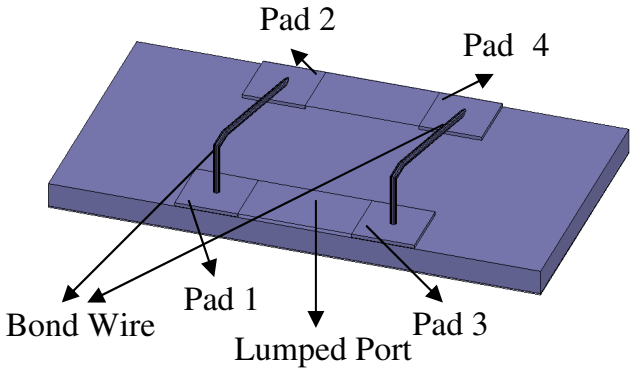

Fig. 11. 3-D Model of two bond wires.

Table 5. Capacitance of two bond wires.

Vertical Distance [µm]	C_{10} [fF]	C_{13} [fF]	C_{12} [fF]	C_{L12} [fF]
300	109.16	28.45	9.98	5.51
400	109.16	18.20	9.98	4.71
500	109.16	13.93	9.98	4.17
600	109.16	11.41	9.98	3.75
700	109.16	9.71	9.98	3.41

System). The comparison of the 3-D simulator results with the circuit model results is shown in Fig. 10. The 3-D simulator results coincide well with the equivalent circuit model results. Reasons for deviations are caused by the different numerical algorithms and different meshing of the various simulation tools. Next two bond wires will be parameterized by varying the distance between them. The distance is varied from 300 µm to 700 µm with a step size of 100 µm. The 3-D field calculations were performed using ANSOFT HFSS. Since differential ports are being used, odd modes arise between the two bond wires.

In order to take this effect into account, some modifications (Pozar, 1998) have to be applied to the equivalent circuit model of the two bond wires (Fig. 12). Due to the odd modes, an E-wall will arise between the two bond wires.

Since the capacitance between the first two pads is C_{13} due to this odd mode, the capacitance between a pad and the E-wall will be $2C_{13}$. This effect has to be taken into account for the capacitance between two bond wires, too. In Fig. 12, this capacitance is separated into three parts, whereas the inductance of the bond wire is separated into two parts. The coupling inductance M between the two bond wires must also be taken into account. The values of these parameters are calculated using ANSOFT Q3-D (Tables 5 and 6).

The pad (GND capacitance C_{10} as well as the bond wire (GND capacitance remains constant. C_{12} and C_{13} describe (Table 5) the capacitance between the pads and C_{L12} is the capacitance between the two bond wires. L_{11} and L_{22} are the inductances of bond wire 1 and bond wire 2 whereas k is their inductive coupling coefficient (Table 6).

5 Conclusions

A parametric modelling concept for the characterization of signal path arrangements of 24 GHz package components for short-range radar applications has been presented in this work. A good agreement between the developed parametric lumped models and 3-D field calculation reference results was found. Furthermore, the possibility to characterize the electromagnetic behaviour of a signal path by interconnec-

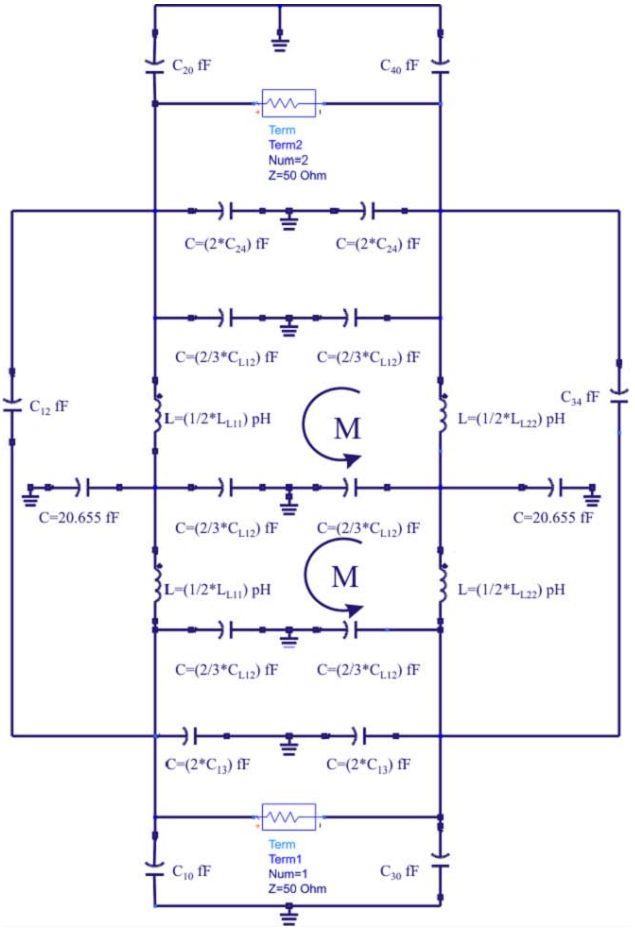

Fig. 12. Equivalent circuit model of two bond wires.

tion of RLC models of the basic signal path elements was shown. Currently, signal path arrangements exhibiting further capacitive and inductive coupling effects are being investigated, to expand the parametric modelling concept.

Acknowledgements. The reported R+D work was carried out in the frame of the BMBF/PIDEA-Project EMCpack/FASMZS (Modelling and Simulation of Parasitic Effects (EMC/SI/RF) for Advanced Package Systems in Aeronautic and Automotive Applications). This particular research was supported by the BMBF (Bundesministerium fuer Bildung und Forschung) of Federal Republic of Germany under grant 16 SV 3295 (Methoden zur zuverlaessigen Systemintegration hochkompakter und kostenoptimaler 24 GHz Radarsensoren für KFZ-Anwendungen im Fahrerassistenzbereich; HF-Entwurf und -Charakterisierung von 24 GHz-Komponenten). The responsibility for this publication is held by the authors only.

In particular we have to thank M. Rittweger (IMST GmbH – Kamp-Lintfort – Germany) supporting us by an EMPIRE research licence; without this support we could not generate all the presented results.

Table 6. Inductance of bond wires.

Vertical Distance [µm]	L_{11} [pH]	L_{22} [pH]	k
300	662.1	151.1	0.228
400	662.3	121.4	0.183
500	665.4	101.2	0.152
600	662.3	86.6	0.131
700	662.2	75.9	0.115

References

Ahn, M.-H., Lee, D., and Kang, S.-Y.: Optimal Structure of Wafer Level Package for the Electrical Performance, IEEE Electronic Components and Technology Conference, 2000.

EMPIRE XCcel Manual: IMST GmbH – Kamp-Lintfort – Germany, 08/2009.

Hussein, H. M. and El-Badawy, E.: An Accurate Equivalent Circuit Model of Flip Chip and Via Interconnects, IEEE MTT-S Digest, 44(12), 2543–2553, 1996.

Ndip, I., Sommer, G., John, W., and Reichl, H.: A Novel Modelling Methodology of Bump Arrays for RF and High-Speed Applications, IMAPS 2003 – 36th International Symposium on Microelectronics; Boston, Massachusetts, USA, 992–997, 2003.

Pozar, D. M.: Microwave Engineering, John Wiley & Sons, 2nd edition, p. 385, 1998.